PHYSICAL REVIEW A VOLUME 37, NUMBER 9 MAY 1, 1988

Above-threshold ionization in helium

P. H. Bucksbaum, M. Bashkansky,* and D. W. Schumacher
AT&T Bell Laboratories, Murray Hill, New Jersey 07974
(Received 13 January 1988)

We report the first high-resolution angle-resolved electron spectra of helium photoionized above threshold by intense, linear, or circularly polarized 532-nm laser pulses. Quantitative comparisons are made to the Keldysh-Faisal-Reiss theory of photoionization in intense fields.

This paper presents the results of high-resolution angle-resolved above-threshold ionization (ATI) in helium by up to 25 photons of 532-nm laser radiation. Although ATI (the absorption of excess photons during multiphoton ionization) has been observed for many atoms,[1] helium is of particular interest, not only because its simplicity permits detailed calculations, but also because it is the most tightly bound neutral atom, and therefore the most difficult to ionize at optical frequencies.

Previous intense-field ionization experiments on helium have been limited to studies of total ion yields or low-resolution angle-integrated electron spectra.[2,3] There is no information about helium ATI peak widths or angular dependence, or on ATI for circularly polarized light. More complete data exist for the heavy rare gases xenon and krypton, which absorb from 2 to 10 excess photons above threshold when ionized by 1064-nm laser light at intensities above 10^3 W/cm^2. Several theories have been proposed that can predict some of these observations,[1] but the quantitative agreement is generally poor, and no current theory explains all the phenomena. The theoretical situation would be aided considerably by the presence of comparably detailed data in the simplest atoms, hydrogen and helium. Some hydrogen ATI spectra and angular distributions for linearly polarized light have recently been measured at rather low intensities ($\leq 10^{12}$ W/cm^2).[4] Here we present the first detailed study of helium, for ATI induced by both linear and circular polarization at intensities of $\approx 10^{14}$ W/cm^2. We also examine the predictions of the Keldysh-Faisal-Reiss (KFR) model of photoionization in intense fields,[5-7] which has successfully described some aspects of ATI in xenon and krypton.[8,9] By carefully measuring all relevant laser-beam parameters, and then averaging the theory over those parameters, we are able to make *quantitative* comparisons to the theoretical rates, spectra, and angular distributions.

The experiments were performed in an evacuated chamber with a base pressure of 4×10^{-9} Torr. Helium atoms were continuously leaked into the chamber to maintain a density in the range of 10^{10} to 5×10^{12} atoms/cm^3. The Fourier-transform-limited laser pulses had a full temporal width at half maximum of 80 ps, and were focused to a Gaussian beam waist with a measured diameter at half maximum of 12 μm. The laser pulse energy could be adjusted between 0 and 35 mJ, so that the peak intensity in the interaction region was as high as 2.5×10^{14} W/cm^2. Photoelectrons were collected by a microchannel plate detector subtending a solid angle of 0.002 sr, placed 40 cm from the laser focus in the plane perpendicular to the laser direction **k**. Electron energies were determined by time-of-flight measurements. The detection efficiency is dominated by the channel plate, and estimated at 10%.

Figure 1 shows a series of ATI spectra collected for linear polarization along the detection axis. At least 11 photons are required to ionize helium ($h\nu=2.33$ eV, ionization potential equal to 24.59 eV), but prominent peaks are only observed for 13 photons or higher. The sharp spectral features below 5 eV are contaminants entering the chamber with the helium gas, and were significantly reduced after baking the gas manifold, as seen in the fourth spectrum from the top.

As the intensity increases the number and width of ATI peaks also increases, in a way that is quite reminiscent of ATI in xenon produced by 1064-nm 100-ps laser pulses.[10] Indeed, xenon also requires at least 11 (1064 nm) photons to ionize, since the ionization potential is about half that of helium.

Spectra, like the ones in Fig. 1, were collected at $\pi/12$ radian increments as the laser polarization was rotated by 2π. The total number of electrons collected in each ATI peak is plotted in Fig. 2, as a function of the azimuthal angle ϕ between the laser polarization and the detection axis.

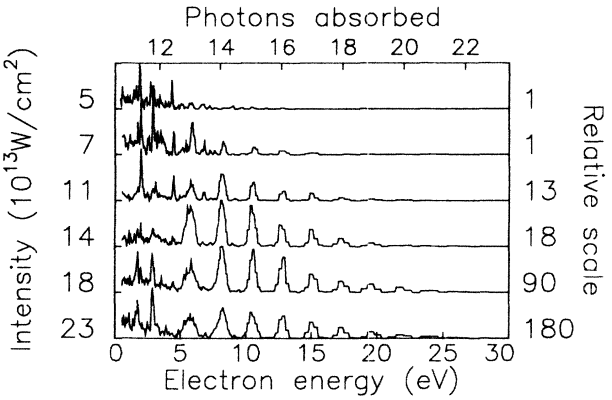

FIG. 1. ATI in helium for linearly polarized 532-nm light, with detection along the polarization direction, for several laser pulse intensities. The number to the left of each spectrum shows the peak intensity in the 80 ps focused laser pulse for that data. The number to the right shows the relative vertical scale for the various spectra. The horizontal axis shows the electron energy in electron volts (bottom) and the number of photons absorbed to produce an electron at the position (top).

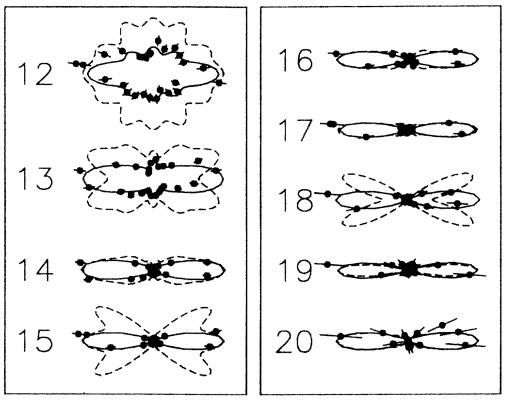

FIG. 2. Photoelectron distributions in the azimuthal plane (perpendicular to the laser direction) for helium ATI peaks corresponding to 12 to 20 photons absorbed. The laser polarization is horizontal in these diagrams. The peak laser intensity is 2×10^{14} W/cm^2. Points are data. The error bars are statistical. The solid lines are empirical fits (see text). Dashed lines are predictions of the KFR theory (see text for details).

(Note that this procedure includes redundancy, since polarization angles separated by π radians are equivalent.) The error bars are 1σ statistical uncertainties. Nonstatistical errors are also present, due to drifts in the laser pulse energy, which was kept within a range of $\pm5\%$. The angular positions include a slight correction for known residual static magnetic fields in the interaction region. The curves through the data are fits to a series of the form

$$f(\phi)=\sum_{n=0}^{5} C_n\cos(2n\phi)\ . \tag{1}$$

The fitting coefficients C_n are shown in Table I. The dotted lines are the predictions of the KFR model, discussed below.

Intense-field calculations involving circular polarization are considerably more tractable than linear polarization, and circular polarization experiments in xenon have proved useful tests of nonperturbative theories of ATI. Until now, however, no circular polarization data existed for hydrogen or helium. Figure 3 shows the ATI spectrum for ionization of helium by circularly polarized light (the top figure). To obtain this spectrum, the chamber and manifold were baked to remove contaminants. The spectrum consists of 30000 laser pulses with helium present, subtracted by a comparable number of pulses with the helium removed, to eliminate contributions from background gas. The bell-shaped distribution of ATI peaks, and the near total suppression of low-energy peaks, are characteristics that were first observed in 1064-nm circularly polarized ATI in xenon.[11] The suppression is thought to be due to a centrifugal barrier to ionization. Briefly, the electron, in absorbing n photons, must also absorb $n\hbar$ units of angular momentum. The outgoing electron wave is therefore excluded from the region close to the nucleus by a repulsive centrifugal effective potential. This reduces the n-photon ionization matrix element. Higher energy ATI electrons, despite their higher angular momentum, can penetrate closer to the nucleus because of their higher kinetic energy. In xenon the most intense peak appeared at 8 eV, six (1064 nm) photons above threshold, whereas in helium the most intense peak is at 20 eV, eight (532 nm) photons above threshold.

TABLE I. Helium angular distributions. Fitting coefficients for Eq. (1).

Photons absorbed	Coefficients C_n					
	C_0	C_1	C_2	C_3	C_4	C_5
12	0.53	0.21	0.11	0.05	0.08	0.02
13	0.41	0.30	0.19	0.05	0.04	0.01
14	0.23	0.33	0.22	0.12	0.07	0.03
15	0.18	0.28	0.22	0.15	0.11	0.06
16	0.19	0.28	0.19	0.17	0.12	0.05
17	0.17	0.26	0.22	0.16	0.12	0.07
18	0.18	0.30	0.22	0.15	0.09	0.06
19	0.17	0.26	0.21	0.17	0.13	0.06
20	0.20	0.30	0.22	0.14	0.07	0.07

In a recent Letter, Reiss showed that the relative peak intensities in the circular polarization spectrum for xenon were in reasonable agreement with the predictions of a modified Keldysh theory (the KFR model) of intense-field ionization.[8] Briefly, that theory approximates the outgoing electron wave by a "Volkov" state, which is a plane-wave electron in an electromagnetic field. The result for k-photon ionization with circular polarization, in the laser plane-wave and electric dipole limit, is particularly simple:

$$\frac{dW_k}{d\Omega}=\frac{\pi}{\hbar}(2m_e)^{3/2}(k\hbar\omega-U_P)^2 \times(k\hbar\omega-U_P+E_0)^{1/2}|\Phi(\mathbf{p})|^2 J_k^2(\beta)\ . \tag{2}$$

Here $\Phi(\mathbf{p})$ is the momentum-space wave function for the atomic ground state, evaluated at the photoelectron's final momentum $p=[2m_e(k\hbar\omega-U_P+E_0)]^{1/2}$ and direction. U_P is the "ponderomotive potential" at the point of ionization, described below. E_0 is the ground-state energy, and $J_k(\beta)$ is a cylindrical Bessel function of order k and argument

$$\beta=2\sin\theta\sqrt{U_P(k\hbar\omega+E_0-U_P)}/(\hbar\omega)\ .$$

θ is the emission angle with respect to the laser wave vector $\mathbf{k}$.

We have performed this calculation for helium, using the Hartree single electron variational $1s$ wave function for the initial state.[12] In order to compare this prediction to the data, the spatial and temporal inhomogeneity of the tightly focused pulsed laser must be considered. These not only contribute to an averaging over different intensities, but more importantly, they cause ponderomotive energy and momentum transfer between the outgoing photoelectron and the laser light. These effects have been thoroughly studied and are now well understood, as follows.

The energy associated with the oscillatory motion of a classical electron in a light field appears on time average as an effective "ponderomotive" potential U_P,[13] equal to

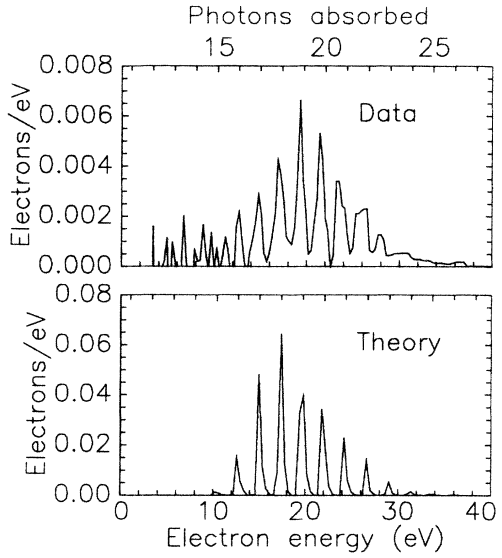

FIG. 3. Top: ATI in helium for circular polarization. The laser peak intensity was 2×10^{14} W/cm^2, and the helium density was 4.5×10^{12} cm^{-3}. Other experimental parameters are given in the text. The vertical scale is calibrated in electrons detected per laser pulse, per eV. Bottom: Prediction of the KFR theory for this experiment, including temporal and spatial averaging, and all final-state scattering.

$2.6[I/(10^{14}$ W/cm$^2)]$ eV for 532-nm radiation. At high laser intensities, this energy becomes comparable to the electron's translational kinetic energy following ionization. The translational energy itself is lowered by $\approx U_P$, due to the ac Stark effect.[14] In addition, scattering from the ponderomotive potential as the photoelectron exits the laser focus greatly alters both the electron's energy[15] and direction.[16]

These effects are included in our calculation, with measured values for the laser focal waist, duration, and intensity profile, and the overall detection efficiency. The results are simulations of the experiment that can be directly compared to the data.

Figure 3 (lower figure) shows the predicted spectrum for circularly polarized light. The vertical axis is calibrated in units of electrons detected per unit energy, during one laser pulse, for the beam parameters and helium density employed in the experiment. The general spectral shape predicted by the KFR theory is similar to the data. In fact, if the peak intensity in the calculation is increased by about 30%, this agreement becomes quite good. This is similar to Reiss's finding[8] that the best agreement between the calculated and observed spectral shape in xenon occurred if the calculation assumed a somewhat higher intensity than was measured. The helium ionization rates, however, disagree by about an order of magnitude.

The same techniques may be employed to simulate the linear polarization data. The rate differs from Eq. (2) by replacing each Bessel function with a sum[6,7]

$$\sum_{m=-\infty}^{\infty} J_m(\alpha)J_{k+2m}(\gamma) ,$$

where

$$\gamma=2\sin\theta\cos\phi\sqrt{2U_P(k\hbar\omega+E_0-U_P)}/(\hbar\omega) ,$$

and $\alpha=U_P/(2\hbar\omega)$. The results, shown in Fig. 4, show reasonable agreement for overall rates, but are not as successful as the circular polarization calculation in reproducing the spectrum.

Finally, the angular distributions for linear polarization are also predicted by Eq. (2). After spatial and temporal averaging over the laser beam, and including the final-state ponderomotive scattering, the calculated angular distributions are shown as the dashed lines in Fig. 2. Although there is good agreement for some electron peaks, the overall agreement is quite poor. Specifically, the calculations show considerably more complex angular structure than the data, which are narrowly directed along the polarization direction for all ATI peaks.

In conclusion, we have presented the first detailed electron spectra for ATI in helium, a system of great importance in assessing various theories of intense field ionization. A direct comparison to a Keldysh-Faisal-Reiss nonperturbative calculation showed reasonable agreement for circular polarization spectra, but rather poor agreement for linear polarization angular distributions and spectra. The agreement with calculated rates is satisfactory, considering that these processes scale as the intensity to the tenth power or more. We are currently investigating helium photoionization with elliptically polarized light, which may be a more sensitive test of the theories. In addition, ionization by subpicosecond pulses, where recent experiments have shown the emergence of an ATI fine structure,[17] would be most interesting.

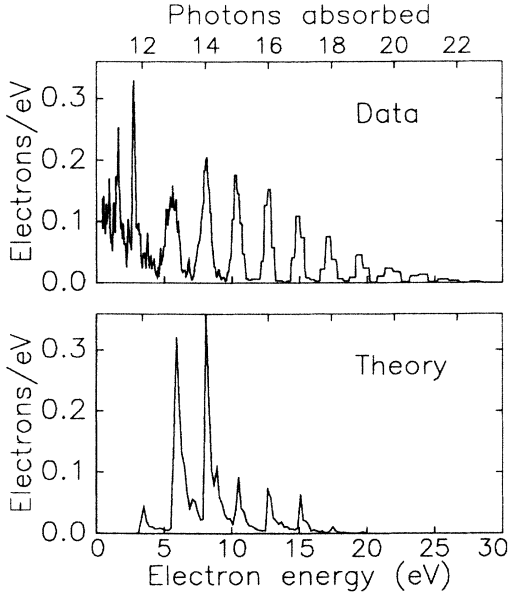

FIG. 4. Top: ATI in helium for linear polarization. The laser peak intensity was 2.3×10^{14} W/cm^2, and the helium density was 6.7×10^{10} cm^{-3}. Bottom: Prediction of the KFR theory for this experiment.

We gratefully acknowledge useful discussions with T. J. McIlrath and R. R. Freeman.

*Also at Physics Department, Columbia University, New York, NY 10027.

[1]See, for example, the feature issue on multielectron excitations in atoms, edited by W. E. Cooke and T. J. McIlrath, J. Opt. Soc. Am. B **4**, 701 (1987).

[2]L. A. Lompre, A. L'Huillier, G. Mainfray, and C. Manus, Phys. Lett. **112A**, 319 (1985).

[3]L. A. Lompre, A. L'Huillier, G. Mainfray, and C. Manus, J. Opt. Soc. Am. B **2**, 1906 (1985).

[4]D. Feldmann, B. Wolff, M. Wemhoner, and K. H. Welge (unpublished).

[5]L. V. Keldysh, Zh. Eksp. Teor. Fiz. **47**, 1945 (1964) [Sov. Phys. JETP **20**, 1307 (1965)].

[6]F. H. M. Faisal, J. Phys. B **6**, L89 (1973).

[7]H. R. Reiss, Phys. Rev. A **22**, 1786 (1980).

[8]H. R. Reiss, J. Phys. B **20**, L79 (1987).

[9]M. Bashkansky, P. H. Bucksbaum, and D. W. Schumacher, Phys. Rev. Lett. **59**, 274 (1987).

[10]T. J. McIlrath, P. H. Bucksbaum, R. R. Freeman, and M. Bashkansky, Phys. Rev. A **35**, 4611 (1987).

[11]P. H. Bucksbaum, M. Bashkansky, R. R. Freeman, T. J. McIlrath, and L. DiMauro, Phys. Rev. Lett. **56**, 2590 (1986).

[12]W. S. Wilson and R. B. Lindsay, Phys. Rev. **35**, 681 (1935).

[13]L. S. Brown and T. W. B. Kibble, Phys. Rev. **133**, A705 (1964).

[14]L. Pan, L. Armstrong, Jr., and J. H. Eberly, J. Opt. Soc. Am. B **3**, 1319 (1986).

[15]P. H. Bucksbaum, M. Bashkansky, and T. J. McIlrath, Phys. Rev. Lett. **58**, 349 (1987).

[16]R. R. Freeman, T. J. McIlrath, P. H. Bucksbaum, and M. Bashkansky, Phys. Rev. Lett. **57**, 3156 (1986).

[17]R. R. Freeman, P. H. Bucksbaum, H. Milchberg, S. Darack, D. Schumacher, and M. E. Geusic, Phys. Rev. Lett. **59**, 1092 (1987).